The Journal of Experimental Biology 209, 455-465
Published by The Company of Biologists 2006
doi:10.1242/jeb.02029

Dynamically similar locomotion in horses

Sharon R. Bullimore* and Jeremy F. Burn

Department of Anatomy, University of Bristol, Southwell Street, Bristol, BS2 8EJ, UK

*Author for correspondence at present address: Human Performance Laboratory, Faculty of Kinesiology, University of Calgary, 2500 University Drive NW, Calgary, Alberta, T2N 1N4, Canada (e-mail: sbullimore@kin.ucalgary.ca)

Accepted 6 December 2005

Summary

It is possible for animals of very different sizes to use the same patterns of locomotion, i.e. to move in a 'dynamically similar fashion'. This will only occur, however, if relevant biomechanical parameters scale with size in such a way that they compensate for the effects of size differences. Here we apply this principle to understanding the effects of size on locomotion within a species: the domestic horse. We predict that, without any factor to compensate for size differences, detectable deviations from dynamically similar locomotion would occur over the size range present in adult horses. We measured relative stride length (RSL) and duty factor (DF) in 21 trotting horses (body mass: 86–714 kg), and interpolated the data to predict RSL and DF at equivalent speeds (Froude numbers: 0.5, 0.75, 1.0). RSL and DF at equal Froude number were not significantly related to body mass. This is consistent with the hypothesis that horses trot in a dynamically similar fashion at equal Froude number. We show that the nonlinear stress–strain relationship of tendon can contribute to reducing deviations from dynamic similarity, 'buffering' the effects of variation in body mass, but conclude that this effect is unlikely to explain fully our results. This suggests that a 'compensatory distortion' may occur in horses, counteracting the effects of size differences. The approach used here is also applicable to understanding the consequences of size changes within an individual during growth.

Key words: ontogeny, allometry, gait, intraspecific, horse, *Equus caballus*.

Introduction

It is possible for animals of very different sizes to use similar patterns of locomotion. For example, kangaroo rats and kangaroos hop bipedally, quails and ostriches walk and run bipedally, and quadrupeds of a wide range of different sizes walk, trot and gallop. A more detailed comparison of locomotion in animals of different sizes can be made by comparing dimensionless parameters, such as stride length divided by leg length ('relative stride length', RSL), stance time divided by stride time ('duty factor', DF), peak ground reaction force (GRF) divided by body weight ('relative peak force', RPF) and the phase relationships of the limbs. Alexander and Jayes (1983) showed that mammalian species of very different sizes use the same values of these dimensionless parameters when moving at speeds corresponding to equal values of another dimensionless parameter, the Froude number (u^2/gh, where u is forward speed, g is the acceleration due to gravity and h is hip height).

All of the dimensionless parameters considered above are 'mechanical' dimensionless parameters, because the parameters from which they are constructed can be defined in terms of forces, lengths and times. Systems that have equal values of mechanical dimensionless parameters are said to be 'dynamically similar' (Isaacson and Isaacson, 1975), so Alexander and Jayes (1983) described animals that have equal values of the above dimensionless parameters as moving in a 'dynamically similar fashion'.

Dynamically similar locomotion is not, however, inevitable in animals moving at equal Froude number. For example, Alexander and Jayes (1983) found that cursorial and non-cursorial mammals do not move in a dynamically similar fashion at equal Froude number and Donelan and Kram (2000) found that humans do not move in a dynamically similar fashion when running at equal Froude number in different levels of simulated reduced gravity. Engineering theory tells us that, for dynamic similarity to occur in some aspect of a system, all relevant system parameters must scale appropriately with size (Isaacson and Isaacson, 1975). Previously, we have applied this to understanding dynamic similarity in animal locomotion. We argued that, because tendon elastic modulus does not increase with size as required for dynamic similarity, compensatory changes in other parameters with size are required for dynamically similar locomotion to be possible (Bullimore and Burn, 2004). We referred to these changes as 'compensatory distortions', after a term that has been used in engineering to describe the

changes that must be made in physical models in order to make them dynamically similar to the systems that they represent (Baker et al., 1973). We showed that the changes in limb posture that occur with size in mammals (Biewener, 1989) should compensate for the size-independence of tendon elastic modulus sufficiently for dynamically similar locomotion to be possible in species of different sizes.

This is an example of a general principle that is frequently encountered in studies of size effects in biology: where organisms of different sizes are made of the same materials, they cannot remain functionally similar unless systematic changes in form compensate for size effects. For example, for animal bones and tree trunks to maintain the same resistance to elastic buckling, their thickness must increase disproportionately with length (McMahon, 1973). Conversely, where form remains the same, differently sized organisms differ functionally. For example, the functional characteristics of the hairy appendages of crustaceans are size-dependent (Koehl, 2004). In the case of mammalian locomotion, changes in limb posture with size allow functional similarity in locomotor mechanics to be maintained despite the size-independence of tendon material properties. However, if no factor compensates for size effects, changes in locomotor patterns with size can be expected, so locomotion will not be dynamically similar.

Size not only varies between species, but also within species. This occurs under two circumstances: (a) between adult individuals, due to genetic and environmental factors, and (b) within an individual during growth. The same principle will apply within species as between species: if tendon elastic modulus is size-independent, and a compensatory distortion does not occur, then individuals of different sizes would not be expected to move in a dynamically similar fashion. This raises two questions. (1) Over the smaller size range present within a species, could the resulting deviations from dynamically similar locomotion be large enough to be detectable and physiologically significant? (2) If so, do systematic deviations from dynamically similar locomotion occur with size within species, or does some factor (a compensatory distortion or a change in tendon elastic modulus with size) prevent this? Answering these questions is important in order to understand the biomechanical consequences of growth and the factors that affect the optimal size for the adults of a species.

Here we address both of these questions for the first circumstance under which intraspecific size differences occur: variation between adult individuals. We chose to study the domestic horse (*Equus caballus*) because it occurs in a wide range of sizes, allowing small deviations from dynamic similarity to be detected, and because there is a large volume of published anatomical and biomechanical literature on this species. To address the question of whether detectable deviations from dynamic similarity could occur (question 1 above), we modelled 'idealised' horses that were identical except for size differences, so that there were no compensatory distortions, and predicted by how much locomotion would deviate from dynamic similarity in these animals. To address the question of whether real horses of different sizes move in a dynamically similar fashion (question 2 above), we measure RSL and DF in trotting horses of body mass 86–714 kg. The theoretical predictions are presented in Part 1 of this paper and the experimental results in Part 2.

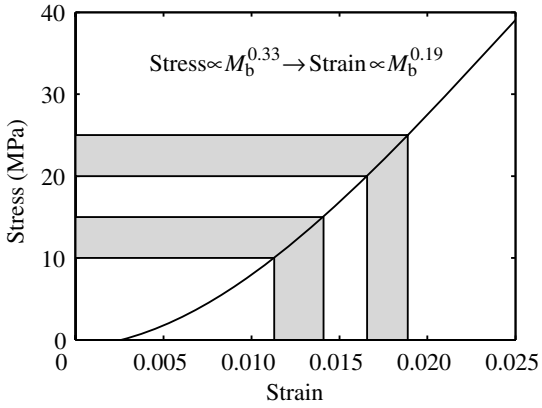

Fig. 1. Consequences of the nonlinear stress–strain relationship of tendon for the scaling of tendon strain. Data of Riemersma and Schamhardt (1985) for equine superficial digital flexor tendon. Because the tendon is stiffer at higher stresses, a given increase in stress causes a smaller increase in strain when it occurs at a higher initial stress (compare shaded regions). A consequence of this is that the scaling exponent for strain is lower than the scaling exponent for stress. For example, over the part of the curve within and between the shaded regions, a stress proportional to $M_b^{0.33}$ causes a strain proportional to $M_b^{0.19}$. Therefore, a nonlinear tendon stress–strain relationship can reduce the effects of size differences on tendon strain.

A factor that could potentially decrease the effects of size on locomotion is the nonlinear stress–strain relationship of tendon. Because tendons are stiffer at higher stresses, a given increase in stress causes a smaller increase in strain when it occurs at higher stresses. A consequence of this is that tendon strain will scale less markedly with size than tendon stress (Fig. 1). If tendon elastic modulus does not increase with size as required for dynamic similarity, and there are no compensatory distortions, then it would be expected that larger animals would experience greater tendon strains, causing deviations from dynamically similar locomotion (Bullimore and Burn, 2004). The capacity of the nonlinear tendon stress–strain relationship to decrease the scaling exponent for strain would reduce this effect. This is not a compensatory distortion, because it does not depend upon something changing with animal size. It also could not compensate completely for a size-independent tendon elastic modulus, because it would never give the same tendon strain for different stresses. However, it could reduce deviations from dynamically similar locomotion to some extent. In order to estimate the magnitude of this effect, we made the predictions in Part 1 both with and without taking these nonlinear tendon properties into account.

(Part 1) Predicted scaling exponents

Two possibilities exist as to the effects of size in horses: (i) there may be no systematic changes with size, or (ii) there may be systematic changes in some parameters with size, for example, in anatomy or muscle activation patterns. In either case, there will also be individual variation due to other factors. Our approach to determining whether size differences could cause detectable deviations from dynamically similar locomotion in the absence of compensatory distortions was to model 'idealised' horses which did not differ in any way except for in size. They therefore had identical muscle activation patterns and tendon properties and were geometrically similar (so all lengths scaled in proportion to $M_b^{0.33}$ and all areas scaled in proportion to $M_b^{0.67}$, where M_b is body mass). This represents situation (i) above, except that variation due to factors other than size is ignored. The relationships of RSL and DF to body mass predicted for these 'idealised' horses were then compared to the relationships measured in real horses in Part 2. A difference between the predicted and measured relationships was taken to indicate that systematic changes with size do occur, i.e. that possibility (ii) above is correct.

The predictions were made in four stages. We first predicted the scaling of tendon strain with size, and used this to estimate the scaling of joint angular excursion. From this, we predicted the scaling of limb stiffness, which we defined as the ratio of peak GRF to limb shortening during the stance phase. Lastly, we used the planar spring-mass model of locomotion to predict how this scaling of limb stiffness would affect RSL, DF and RPF. We made the predictions for both a linear tendon stress–strain relationship and a realistic nonlinear relationship, in order to determine how much this would affect deviations from dynamic similarity.

In order to predict limb stiffness, i.e. in stages (i) to (iii) of the predictions below, we took peak GRF to be proportional to M_b in horses moving at equal Froude number. In horses that are not moving in a dynamically similar fashion, peak GRF will not be exactly proportional to M_b. However, because the force–length relationships of the limbs of animals tend to be approximately linear (Farley et al., 1991; McGuigan and Wilson, 2003), limb stiffness is not sensitive to the GRF for which it is calculated. The scaling exponents predicted below for RPF are small (Table 1), justifying this approximation.

We also assumed that peak tendon force would be proportional to peak GRF, and therefore also to M_b. Again, this assumption will only be exact for dynamically similar horses. If larger horses experience greater joint angular excursions, as expected if tendon elastic modulus is size-independent and there are no compensatory distortions, the moment arms of the GRF about the limb joints will be relatively greater. This will increase the tendon forces required to counteract a given GRF and so could potentially increase deviations from dynamic similarity. From this point of view, the predictions made here are conservative.

(i) Predicted scaling of tendon strain

For a peak tendon force proportional to M_b, and a tendon cross-sectional area proportional to $M_b^{0.67}$, tendon stress will increase with size in proportion to $M_b^{0.33}$. For tendons with a linear stress–strain relationship, strain will scale in proportion to stress and therefore also to $M_b^{0.33}$. In order to predict the scaling exponent for strain in tendons with a nonlinear stress–strain relationship, we used the data of Riemersma and Schamhardt (1985), digitised from their fig. 4. This gives stress–strain relationships for a superficial digital flexor tendon (SDFT), a deep digital flexor tendon (DDFT) and a suspensory ligament (SL) from an equine hindlimb. These structures cross the metacarpophalangeal joint in the forelimb and the metatarsophalangeal joint in the hindlimb. Hyperextension of these joints is responsible for a large proportion of the shortening of the limb during the stance phase in trotting horses (McGuigan and Wilson, 2003) and, because the muscle fibres associated with these structures are relatively short (Ker et al., 1988), it is likely that most of this hyperextension occurs through tendon elongation. Therefore, the properties of these tendons have a substantial influence on overall limb compliance. To determine whether the data of Riemersma and Schamhardt (1985) were typical we fitted straight lines to the stress–strain relationships between strains of 3.5% and 6.5% (R^2>0.99). This gave elastic moduli of 1.15 GPa, 1.44 GPa and 0.56 GPa and intercepts with the strain axis of 1.6%, 2.1% and 2.1%, for the SDFT, DDFT and SL, respectively. Comparison with published values indicated that these are typical properties for mammalian tendons: mean elastic modulus for mammalian limb tendons is 1.24±0.23 GPa (Pollock and Shadwick, 1994) and mean intercept strain for the equine SDFT is 1.5% (Wilson, 1991). In order to make predictions for horses with identical tendon material properties, we used the stress–strain relationships measured by Riemersma and Schamhardt (1985) for horses of all sizes.

The relationship between the scaling exponents for stress and strain depends upon which part of the tendon stress–strain relationship is used. Biewener (1998) calculated peak tendon stresses of approximately 16, 20 and 13 MPa in the SDFT, DDFT and SL, respectively, in trotting horses of approximately 275 kg. We used these values as a starting point for calculating the scaling exponent for strain, which corresponds to a stress proportional to $M_b^{0.33}$. Tendon stresses for horses between 80 and 800 kg were predicted using the equation:

$$\text{stress} = kM_b^{0.33}, \quad (1)$$

where the scaling constant, k, was calculated from the above stresses for a 275 kg horse, giving values of 2.46, 3.08 and 2.00 for the SDFT, DDFT and SL, respectively. The tendon stress–strain data of Riemersma and Schamhardt (1985) were fitted with third order polynomials (R^2>0.99) and these were used to predict tendon strains corresponding to the stresses predicted by Eqn 1. Allometric equations relating these predicted strains to body mass were obtained by log-transforming the data and fitting linear least-squares regression equations (R^2>0.99), as described by Schmidt-Nielsen (1984). This gave scaling exponents of 0.19, 0.16 and 0.18 for strain in the SDFT, DDFT and SL, respectively. To determine how

robust these predictions were, we varied the stresses used for calculating k. Large variations (±5 MPa) altered the predicted exponents by less than 0.01. The predicted exponents are considerably lower than the exponent of 0.33 for a tendon with linear properties, indicating that nonlinear tendon properties could substantially reduce the effects of size on tendon strain.

(ii) Predicted scaling of joint angular excursion

If the joint is modelled as having a circular profile, the joint angular excursion arising from a given tendon strain can be calculated as:

$$\text{angular excursion} = \frac{\text{tendon elongation}}{\text{joint radius}} = \frac{\text{tendon strain} \cdot \text{tendon length}}{\text{joint radius}} . \quad (2)$$

For geometrically similar horses, joint radii and tendon lengths will be proportional to $M_b^{0.33}$, so that joint angular excursions will be directly proportional to tendon strain. Therefore, we take joint angular excursion to be proportional to $M_b^{0.33}$ for a tendon with linear properties and to $M_b^{0.18}$ (the mean of the scaling exponents calculated above) for a tendon with nonlinear properties. In both cases this represents an increase in joint angular excursion with size, but the predicted increase is substantially smaller for a tendon with nonlinear properties.

The above calculation ignores the contribution of muscle strain to joint angular excursion. This seems reasonable in trotting horses because most of the length change in the limb occurs distally (McGuigan and Wilson, 2003) where the muscle-tendon units have relatively short fibres and long tendons (Ker et al., 1988). However, muscle strains would also be expected to increase with size, by the following argument. Muscle stress would increase with size in the same way as tendon stress, i.e. as $M_b^{0.33}$. The horses we are modelling have identical muscle activation patterns. Therefore, due to the nature of the force–velocity relationship of muscle, these higher stresses would tend to decrease the ability of the muscle to shorten and to increase the possibility of it lengthening, resulting in greater muscle strains in larger animals.

(iii) Predicted scaling of limb stiffness

In order to predict the scaling of limb stiffness, we needed to be able to predict limb shortening from joint angular excursion, where limb shortening is defined as the change in the distance between the proximal and distal ends of the limb between ground contact and midstance. This cannot be done without knowledge of limb morphology because the relationship depends upon limb segment lengths and initial joint angles. For this reason, we used experimental data from three horses (horses 7 and 8 from Table 2 and a third horse of 630 kg) as a basis for predicting the scaling exponent for limb shortening. Reflective markers were placed over the joint centres of the right fore- and hindlimbs and their positions were recorded by optical motion capture (240 frames s^{-1}; Proreflex, Qualisys, Sweden) during trot. The marker positions were used to calculate the limb segment lengths, joint angles at ground contact and joint angular excursions between ground contact and midstance. Each leg of each horse was then used separately as the basis for calculating scaling exponents for limb shortening. Limb segment lengths for horses of 80, 200, 400, 600 and 800 kg were predicted by scaling the measured lengths in proportion to $M_b^{0.33}$ (so that they were geometrically similar), and joint angular excursions were predicted by scaling measured values in proportion to $M_b^{0.33}$ to model a tendon with linear properties, or to $M_b^{0.18}$ to model a tendon with nonlinear properties, as predicted above. Limb shortening was then calculated trigonometrically, assuming initial joint angles were equal to measured values. This produced a total of twelve sets of values for predicted limb shortening against M_b: six corresponding to the fore- and hindlimbs of each of the three horses for linear tendon properties, and another six for nonlinear tendon properties. For each of these twelve datasets, an allometric equation relating predicted limb shortening to body mass was calculated by log-transforming the data and fitting a linear least-squares regression equation (R^2>0.99). Because the calculated scaling exponents were very similar for the data based on the three different horses, and on the fore- and hindlimbs, the means of these scaling exponents were used. The mean exponent for limb shortening with linear tendon properties was 0.77±0.01 (± s.e.m.) which, in combination with a GRF proportional to M_b, gives a limb stiffness proportional to $M_b^{0.23}$. The mean exponent for limb shortening with nonlinear tendon properties was 0.58±0.01 (± s.e.m.), which gives a limb stiffness proportional to $M_b^{0.42}$. Therefore, the predicted scaling exponent for limb stiffness is higher with nonlinear tendon properties, but is still substantially lower than the exponent of 0.67 that would be required for dynamic similarity (Bullimore and Burn, 2004).

(iv) Predicted scaling of dimensionless locomotor parameters

The effect of the above scaling of limb stiffness on the dynamics of locomotion was predicted using the planar spring-mass model (Blickhan, 1989; McMahon and Cheng, 1990). This is a simple model of running gaits, such as trot, in which the animal is represented by a point mass bouncing on a spring. It describes the mechanical relationships between basic locomotor parameters such as limb stiffness, stride length, stance time and GRF, and has been shown to be able to model the mechanics of trotting in mammalian species of a wide range of different sizes remarkably well (Farley et al., 1993).

GRF data (1000 Hz; model 9287 force plate, Kistler Instruments, Switzerland) and kinematic data (240 frames s^{-1}; Proreflex) from one horse of intermediate size (horse 8; Table 2) were used to determine model parameter values representative of a horse trotting at Froude numbers of 0.5, 0.75 and 1.0. With the calculated parameter values, the model predicted RSL, DF and RPF to within 5% of the values measured in this horse. Parameter values representing horses of 80, 200, 400, 600 and 800 kg were generated by scaling limb stiffness as calculated above (i.e. in proportion to $M_b^{0.23}$ for

linear tendon properties and to $M_b^{0.42}$ for nonlinear properties) and keeping the other model parameters dynamically similar to the values calculated for horse 8. The parameter values that were used are listed in the Appendix. Predictions of RSL, DF and RPF for the horses of different sizes were then obtained by numerical integration of the equations of motion for the model using a function written in Matlab (version 6.5, The MathWorks, Inc., MA, USA). The method used has been described in detail previously (Bullimore and Burn, 2006). Allometric equations relating the predicted values of RSL, DF and RPF to body mass were obtained by log-transforming the data and fitting linear least-squares regression equations (R^2>0.98). The scaling exponents predicted for both linear and nonlinear tendon properties are shown in Table 1. The exponents for RSL and DF are positive, indicating that these dimensionless parameters are predicted to increase with size, while the exponents for RPF are negative, indicating that it is predicted to decrease with size. Incorporating the nonlinear characteristics of tendon into the predictions substantially reduced the exponents predicted for RSL, while the exponents predicted for DF and RPF were small for both linear and nonlinear tendon properties.

Table 1. *Predicted scaling exponents for the relationships of relative stride length, duty factor and relative peak force to body mass in 'idealised' horses that are identical except for size differences*

	Froude number	Predicted scaling exponent	
		Linear tendon	Nonlinear tendon
RSL	0.50	0.19	0.11
	0.75	0.17	0.10
	1.00	0.16	0.09
DF	0.50	0.03	0.01
	0.75	0.04	0.02
	1.00	0.05	0.03
RPF	0.50	–0.02	–0.01
	0.75	–0.04	–0.02
	1.00	–0.05	–0.02

RSL, relative stride length; DF, duty factor; RPF, relative peak force.

Predictions were made for both a linear and a nonlinear tendon stress–strain relationship.

In summary, the results obtained in Part 1 predict that: (a) in horses that do not exhibit any systematic changes with size, RSL at equal Froude number will increase with size in proportion to approximately $M_b^{0.10}$, while DF and RPF will be close to independent of size, and (b) relative to a tendon with a linear stress–strain relationship, a tendon with a realistic nonlinear relationship could reduce the effects of size on tendon strain, joint angular excursion and RSL.

(Part 2) Measured scaling exponents

Materials and methods

Overview

RSL and DF were measured in 21 adult horses *Equus callabus* (86–714 kg, Table 2) trotting at a range of speeds. The data for each horse were interpolated to predict the RSL and DF that the horse would use at Froude numbers of 0.5, 0.75 and 1.0. Dynamic similarity of RSL and DF was defined as these parameters being independent of body mass in horses trotting at equal Froude number.

Anatomical measurements

Girth was defined as the circumference of the trunk just behind the forelegs. Wither height was defined as the height above the ground of the highest point at the base of the neck. Body mass was measured using a weighbridge, girth was measured using a tape measure and the height of the withers and the greater trochanter above the ground were determined using a measuring stick.

To calculate RSL and Froude number, a measure of leg length is required. Previous studies (e.g. Alexander and Jayes, 1983; Donelan and Kram, 2000) used greater trochanter height in the standing animal. However, the greater trochanter is difficult to palpate in horses and its height above the ground varies with standing posture. Preliminary calculations based on a pilot study indicated that error in this measurement was likely to be a significant source of interindividual variability. Therefore, instead we measured radius and metacarpus length between the most distal prominence on the lateral side of the elbow joint and the prominence on the lateral, proximopalmar aspect of the proximal phalanx. This measurement proved to be substantially more repeatable than greater trochanter height. For convenience, we multiplied the measured radius and metacarpus lengths by a scale factor of 2.05 to obtain a 'calculated leg length', which was approximately equal to greater trochanter height. This was done to make our results comparable with previous studies. The scale factor of 2.05 was the mean value of the ratios of greater trochanter height to radius and metacarpus length for all the horses. This ratio was independent of body mass (Table 3). Because the same scale factor was used for all horses it did not contribute to interindividual variability and so did not affect the capacity to detect deviations from dynamic similarity. The calculated leg lengths are shown in Table 2.

Experimental procedure

All experimental procedures were approved by the University ethics committee. Reflective markers were attached to the medial side of the left fore hoof, to the lateral side of the right fore hoof and overlying the dorsal spinous process of the fifth thoracic vertebra ('t5 marker'). The horses were trotted along a track by an experienced handler. The first section of the track was used for acceleration, the central section for data collection and the final section to slow the horses to a stop. The positions of the reflective markers were recorded at 240 frames s^{-1} using a 3D optical motion capture system (Proreflex) as the horses passed through the data collection

region. The field of view was sufficient for at least one stride to be recorded from all horses at all speeds. For all except horses 7 and 8, one stance phase of the left or right fore leg was recorded at 250 frames s^{-1} using a high speed digital video camera (MotionCorder SR-1000, Kodak, Herts, UK). Trials were obtained over as wide a range of trotting speeds as possible while maintaining an approximately constant speed through the data collection region.

Data analysis

Allometric equations relating girth, wither height, greater trochanter height and radius and metacarpus length to body mass were calculated by log-transforming the data and fitting linear regression lines. Reduced major axis (RMA) regression was used because this method is appropriate for data in which error occurs in both the dependent and independent variables (Rayner, 1985). The fit of the allometric equations was assessed by calculating the mean absolute percent deviation (MAPD) of the data from the values predicted by the equations (Prothero, 1986). 95% confidence intervals for the scaling exponent were calculated using the t-distribution. If these confidence intervals included 0.33, the horses were considered to be geometrically similar in the measurement in question (Schmidt-Nielsen, 1984). The ratio of greater trochanter height to radius and metacarpus length was calculated and an allometric equation relating this parameter to body mass was calculated as above, except that least-squares regression was used because the relationship obtained using RMA regression did not fit the data well, probably because the range of the dependent variable was small.

Forward speed was calculated as the mean velocity of the t5 marker over one complete stride. Stride length was calculated as the distance travelled by the left or right fore-hoof marker between consecutive stance phases of that hoof. Stance time was determined from the high speed video. Stride time was calculated as stride length divided by forward speed. RSL was calculated as stride length divided by calculated leg length, DF was calculated as stance time divided by stride time and Froude number was calculated as u^2/gh, where u is forward speed, g is the acceleration due to gravity (9.81 m s^{-2}) and h is calculated leg length.

For each horse, the RSL and DF that would be used at Froude numbers of 0.5, 0.75 and 1.0 were predicted by fitting quadratic equations to the data for RSL and DF against Froude number. Quadratics were chosen on the basis of a pilot study in six horses in which linear, quadratic, power and logarithmic functions were tested and quadratics gave the highest R^2 values. Higher order polynomials were not used, despite sometimes giving higher R^2 values, because the resulting curves often exhibited multiple extrema, which were thought unlikely to be representative of the true relationship.

For each of the three Froude numbers considered, allometric equations relating RSL and DF to body mass were calculated as described above. Least-squares regression was used because RMA regression gave a poor fit to the data. MAPD and 95% confidence intervals were calculated as described above. If the confidence intervals included zero, the parameter in question was considered to be independent of body mass and therefore to be dynamically similar.

Table 2. *Horses used in the study in descending order of body mass*

No.	Breed	Body mass (kg)	Calculated leg length (m)	Speed range (m s^{-1})	Number of trials
1	ID	714	1.44	2.18–4.14	15
2	TB×ID	712	1.49	2.50–4.07	14
3	Warmblood	664	1.46	2.43–4.18	13
4	Warmblood	654	1.47	2.54–4.76	14
5	TB type	608	1.49	2.06–4.08	14
6	TB	594	1.48	2.30–4.28	14
7	TB	518	1.38	2.12–3.82	10
8	TB	511	1.40	2.59–3.73	10
9	Arab	418	1.31	2.03–4.25	15
10	New Forest	354	1.10	1.93–3.45	15
11	Unknown	348	1.08	1.66–4.21	15
12	Arab×Welsh	314	1.10	2.16–3.99	15
13	Welsh B	294	1.17	1.95–4.16	16
14	Welsh A	279	1.04	1.95–4.30	13
15	Welsh×unknown	277	1.13	2.06–4.45	15
16	Unknown	266	1.02	2.16–3.82	16
17	Welsh A	240	1.04	1.94–4.66	14
18	Falabella	161	0.72	1.73–3.38	14
19	Falabella	125	0.71	1.59–3.48	16
20	Miniature Shetland	93	0.61	1.65–3.33	14
21	Falabella	86	0.63	1.76–3.12	15

ID, Irish Draught; TB, Thoroughbred.

Table 3. *Allometric equations relating anatomical measurements to body mass in horses used in the study*

	a	b	95% CL		MAPD (%)
			Lower	Upper	
Including horses 18–21					
Wither height	0.11	0.43	0.39	0.48	4.63
Radius and metacarpus length	0.04	0.45	0.41	0.49	4.62
Girth	0.26	0.32	0.30	0.34	2.17
Greater trochanter height	0.09	0.44	0.40	0.49	4.99
GT/RMC	2.13	–0.01	–0.04	0.02	3.28
Excluding horses 18–21					
Wither height	0.14	0.39	0.32	0.46	3.85
Radius and metacarpus length	0.06	0.38	0.32	0.46	3.85
Girth	0.20	0.35	0.32	0.38	1.74
Greater trochanter height	0.11	0.40	0.33	0.49	4.46
GT/RMC	1.83	0.02	–0.04	0.07	3.04

Equations are of the form: measurement=aM_b^b, where M_b is body mass in kg.
CL, confidence limits for the scaling exponent, b.
MAPD, mean absolute percent deviation of measured values from the fitted relationship.
All anatomical measurements are defined in Materials and methods.
GT/RMC = ratio of greater trochanter height to radius and metacarpus length.
All measurements are in m (GT/RMC in m/m).
Relationships are given both excluding and including data for horses 18–21.

Table 4. *Allometric equations relating relative stride length and duty factor to body mass in horses trotting at equal Froude number*

	Froude number	a	b	95% CL		MAPD (%)
				Lower	Upper	
RSL						
Including horses 18–21						
	0.50	1.43	0.00	–0.04	0.03	3.7
	0.75	1.49	0.01	–0.02	0.04	3.3
	1.00	1.66	0.01	–0.01	0.04	3.1
Excluding horses 18–21						
	0.50	1.30	0.01	–0.04	0.07	3.4
	0.75	1.37	0.03	–0.03	0.08	3.2
	1.00	1.61	0.02	–0.03	0.07	3.1
DF						
Including horses 18–21						
	0.50	0.47	0.00	–0.03	0.03	2.5
	0.75	0.44	–0.01	–0.04	0.03	3.5
	1.00	0.39	0.00	–0.03	0.04	3.7
Excluding horses 18–21						
	0.50	0.41	0.02	–0.03	0.08	2.5
	0.75	0.38	0.02	–0.04	0.08	3.5
	1.00	0.32	0.04	–0.02	0.10	3.2

RSL, relative stride length; DF, duty factor.
Equations of the form: RSL or DF=aM_b^b, where M_b is body mass in kg.
CL, confidence limits for the scaling exponent, b.
MAPD: mean absolute percent deviation of measured values from the fitted relationship.
Relationships are given both including and excluding data for horses 18–21.

Results

The allometric equations calculated for the anatomical measurements are given in Table 3. The four smallest horses (horses 18–21) had relatively short legs for their mass so that, when all horses were included in the analysis, the scaling exponents for wither height, greater trochanter height and radius and metacarpus length were significantly higher than would occur in geometrically similar animals. Only the exponent for girth was not significantly different from 0.33. When these horses were excluded from the analysis, the scaling exponents for wither height, radius and metacarpus length and girth were not significantly different from 0.33, indicating that the other horses were geometrically similar in these parameters. The scaling exponent for greater trochanter height was still significantly greater than 0.33 (P=0.045), however. To determine the effect of the proportionally shorter legs of horses 18 to 21, the relationships of RSL and DF to body mass were determined both with and without the data for these horses.

The number of trials and range of speeds obtained for each horse are shown in Table 2. The Froude numbers at which comparisons were made were well within the range of speeds achieved by all but one of the horses (horse 10), which only reached a Froude number greater than 1.0 in one trial, while all the other trials were at Froude numbers of 0.80 or slower. This horse was excluded from the analysis at a Froude number of 1.0, but was included in the rest of the analysis. The quadratic equations were a good fit to the relationships of RSL to Froude number, with R^2 values between 0.95 and 1.00. The data for DF showed more scatter around the fitted lines, with R^2 values between 0.60 and 0.98.

At all three of the Froude numbers considered, the scaling exponents for RSL and DF against body mass were not significantly different from zero (Fig. 2, Table 4). This conclusion was not altered by including horses 18–21 in the analysis. Including data from these horses increased the body mass range without greatly increasing the scatter of the data, so resulted in narrower confidence intervals (Table 4). The results support the hypothesis that RSL and DF are independent of size in horses and therefore that these parameters are dynamically similar in horses trotting at equal Froude number.

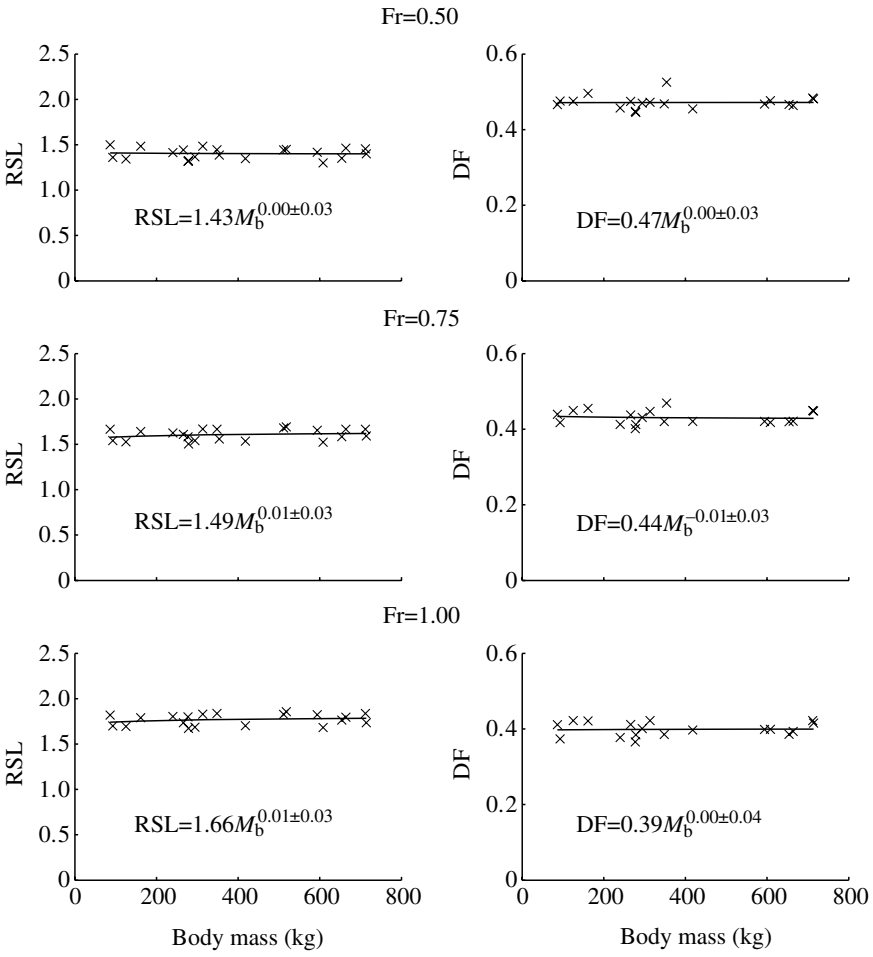

Fig. 2. Relationships of relative stride length (RSL) and duty factor (DF) to body mass (M_b) in horses trotting at three different Froude numbers (Fr). Allometric equations describing the data are shown (scaling exponents given ± 95% confidence intervals) and are indicated by the solid lines. The scaling exponents were not significantly different from 0, indicating that RSL and DF are independent of body mass in horses trotting at equal Froude number.

Discussion

The first question that we addressed was whether detectable and physiologically significant deviations from dynamic similarity could occur over the size range present within a species. When the nonlinearity of the tendon stress–strain relationship was taken into account in the theoretical predictions, RSL was predicted to scale in proportion to approximately $M_b^{0.10}$ (Table 1). This illustrates the argument that we have made previously that dynamically similar locomotion would not be expected in geometrically similar animals with identical tendon properties (Bullimore and Burn, 2004). The scaling exponent of 0.10 is well outside the 95% confidence intervals that we obtained experimentally when all horses were included in the analysis (Table 4), so would have been detectable in our experimental measurements (Fig. 3). This suggests that detectable deviations from dynamically similar locomotion are possible over the size range present in adult horses.

Horses have been bred by humans to occur in a wider range of sizes than the adults of most wild species. Over a narrower size range, the scaling exponent

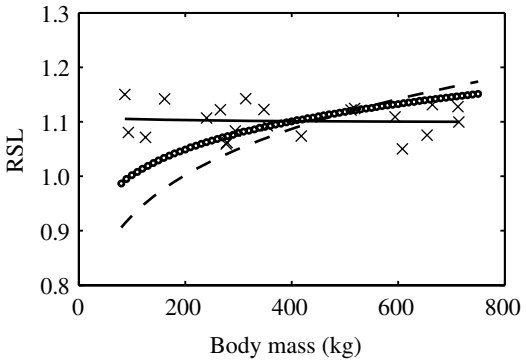

Fig. 3. Measured and predicted relationships of relative stride length (RSL) to body mass (M_b) in horses trotting at a Froude number of 0.5. Crosses are measured values, solid line is allometric equation fitted to measured values ($RSL \propto M_b^{0.00\pm0.03}$), broken line is relationship predicted with linear tendon properties ($RSL \propto M_b^{0.19}$), circles are relationship predicted with realistic nonlinear tendon properties ($RSL \propto M_b^{0.11}$). The predicted effect of size is substantially reduced by taking into account the nonlinear properties of tendon, but is still greater than measured experimentally. This suggests that additional factors compensate for size effects in horses.

of 0.10 predicted for RSL would not be detectable over inter-individual variation. For example, if RSL was 1.50 in an animal of 400 kg, a scaling exponent of 0.10 would give an RSL of 1.55 in a 550 kg individual. This difference is smaller than the differences that would occur between individuals of the same size given a MAPD of 3.5% as measured here. This suggests that, with a nonlinear tendon stress–strain relationship, locomotion would not deviate sufficiently from dynamic similarity to be detectable, or physiologically significant, among the adult members of many species.

In this study, we have only considered the consequences of size differences between adult individuals. However, the size changes that occur during growth are often much greater. Therefore, it seems likely that detectable alterations in locomotion could arise within an individual during growth. It would be of interest to determine whether this occurs and to identify the biomechanical consequences. In addition to the effects of size, locomotion will also be influenced by changes in anatomical proportions and tendon properties during growth. For example, the increase in tendon elastic modulus that occurs with age in some species (Gillis et al., 1995; Yamamoto et al., 2004) may allow dynamically similar locomotion to be maintained despite large size differences.

The question of the physiological significance of the predicted deviations from dynamic similarity is more difficult to answer. A useful first approach is to compare the magnitude of the predicted size effects with the amount of interindividual variability that arises from other sources. The values of RSL that we measured at a Froude number of 0.75 ranged between 1.50 and 1.69, although some of this variability probably arose from experimental error. With a scaling exponent of 0.10, mean RSL would increase from 1.50 to 1.85 over the size range of horses used in this study. This effect is larger than the measured interindividual variability, so could potentially be physiologically significant.

The scaling exponents predicted for DF and RPF, both with and without taking nonlinear tendon properties into account, were very low. This indicates that these parameters are unlikely to vary much with size, even without compensatory distortions, and that they are insensitive to the scaling of leg stiffness. This may explain why Alexander and Jayes (1983) found greater differences in RSL than in DF when comparing mammalian species of different sizes. Because the exponents predicted for these parameters were within, or close to, our measured confidence intervals, we could not distinguish them statistically from zero.

The second question that we addressed was whether systematic deviations from dynamically similar locomotion occur with size in adult horses. We found that the scaling exponents for RSL and DF in horses trotting at equal Froude number were not significantly different from zero. The 95% confidence intervals for the scaling exponents were narrow (Table 4), indicating that any deviations from dynamic similarity that occur in RSL and DF are likely to be very small. We did not measure the phase relationships of the limbs or the RPF. However, all of the horses were trotting, so their diagonal limb pairs must have had a phase difference of half a stride. Griffin et al. (2004) have also shown that the abrupt change in limb phase at the walk–trot transition occurs at similar Froude numbers in horses of different sizes, as would occur in dynamically similar locomotion. It can be deduced that RPF must have been close to independent of size because, if vertical GRF rises and falls as a half sinusoid during the stance phase, animals moving with equal DF must also have equal RPF (Alexander et al., 1979). Vertical GRF is approximately sinusoidal in horses (Witte et al., 2004), and we found that DF was independent of size, so RPF must have been independent, or close to independent, of size.

Our results are therefore consistent with the hypothesis that horses of different sizes move in a dynamically similar manner when trotting at equal Froude number. This does not necessarily imply that the same would be found in an undomesticated species that is subject to natural selection. However, it does show that dynamic similarity in RSL and DF is possible within a species over a more than eightfold range of body mass. Because we only considered trotting, further work would be needed to establish whether horses of different sizes move in a dynamically similar manner at other gaits. It is also important to note that dynamic similarity in some mechanical parameters cannot be taken to imply that other mechanical parameters are dynamically similar (Bullimore and Burn, 2004).

We predicted theoretically that, in ‘idealised’ horses which were identical except for size differences, RSL at equal Froude number would increase with size. However, we did not find this experimentally; the measured scaling exponents were significantly different from the theoretically predicted values and were not significantly different from zero. This discrepancy suggests that some systematic change

occurs with size in horses that compensates for the effects of size differences on locomotion. It would be of interest to identify this factor. One possibility is that, while tendon elastic modulus does not increase with size across species (Pollock and Shadwick, 1994), it does increase with size in horses. Alternatively, a compensatory distortion may occur. For example, larger horses may have relatively thicker tendons. We have discussed possible sites of compensatory distortions previously (Bullimore and Burn, 2004) and concluded that an important compensatory distortion between species is the scaling of the effective mechanical advantage (EMA) of the limb (Biewener, 1989). Large animals tend to have a more upright limb posture than smaller species, and Biewener (1989) demonstrated that this results in a systematic increase the ratio of muscle moment arms to GRF moment arms (the EMA) with animal size. This compensates for the size-independence of tendon elastic modulus in three ways: (i) by decreasing the muscle and tendon forces required to counteract a given GRF, (ii) by decreasing the joint angular excursion that arises from a given tendon elongation, and (iii) by decreasing the limb shortening that arises from a given joint angular excursion. Griffin et al. (2004) have shown that no gross changes in limb posture occur with size in horses. However the changes in EMA that would be required to maintain dynamically similar locomotion in horses would be small and therefore difficult to detect. To illustrate this, the metacarpophalangeal joint can be taken as an example. In a 450 kg horse, the digital flexors have a moment arm about this joint of approximately 30 mm (Brown et al., 2003) and the GRF moment arm at midstance is approximately 100 mm (S.R.B. and J.F.B., unpublished data). If EMA is independent of size, and muscle moment arms scale in proportion to $M_b^{0.33}$, then the corresponding GRF moment arms would be 57 mm in an 80 kg horse and 116 mm in a 700 kg horse, while the muscle moment arms would be 17 mm and 35 mm, respectively. However, a small change in muscle moment arms, to 11 mm and 39 mm respectively, would give an EMA that was proportional to $M_b^{0.26}$, as has been found between species (Biewener, 1989). This is a difference of only a few millimetres, suggesting that careful measurements from a large number of individuals would be required to detect it.

An important question is how such a compensation for the effects of size could occur in a species where the size range has developed through artificial selection by humans. Horses are often used for physically demanding activities and are selectively bred for a wide range of characteristics including speed, endurance, agility and resistance to injury. The fact that this has resulted in similar patterns of locomotion being maintained across a wide range of sizes suggests that this way of moving confers desirable qualities. The lack of even a small amount of locomotor scaling with size suggests that relatively slight alterations in movement would be detrimental. Similarly, the (different) selection pressures acting on wild species could potentially also result in dynamically similar locomotion by selecting for optimal locomotor patterns.

Our third aim was to estimate the extent to which nonlinear tendon properties could compensate for the effects of size. We found that taking nonlinear tendon properties into account substantially reduced the scaling exponents predicted for tendon strain, joint angular excursion and RSL, so that predicted deviations from dynamic similarity were smaller than for linear tendon properties. These predictions were made for horses, but tendon properties are similar among species (Pollock and Shadwick, 1994), and the tendons of many species are loaded predominantly in the nonlinear region of their stress–strain relationships (Ker et al., 1988). Therefore these conclusions are likely to be widely applicable. The effect of tendon nonlinearity will be greatest when tendons are used in the low stress region, where the stress–strain relationship is at its most nonlinear. Therefore we expect the effect of tendon nonlinearity to decrease as speed increases during locomotion. Because the digital flexor tendons of horses are loaded at higher stresses than many other tendons (Ker et al., 1988), we also expect the effect of nonlinear tendon properties to be greater in many other species and tendons than was found here. Where tendons are used at low stresses, their nonlinear properties will effectively help to ‘buffer’ the effects of size differences on locomotion. In addition to reducing locomotor differences between individuals, this could also reduce the effects of body mass fluctuations within an individual due to, for example, growth, pregnancy or seasonal variation.

Table A1. *Spring-mass model parameter values used to model horses of different sizes trotting at equal Froude number (Fr)*

Body mass	*Fr*=0.5				*Fr*=0.75				*Fr*=1.0			
(kg)	K_{lin}	K_{nonlin}	U_0	V_0	K_{lin}	K_{nonlin}	U_0	V_0	K_{lin}	K_{nonlin}	U_0	V_0
80	40.72	28.63	0.71	0.05	40.72	28.63	0.87	0.08	40.72	28.63	1.00	0.09
200	27.29	22.84	0.71	0.05	27.29	22.84	0.87	0.08	27.29	22.84	1.00	0.09
400	20.17	19.25	0.71	0.05	20.17	19.25	0.87	0.08	20.17	19.25	1.00	0.09
600	16.89	17.42	0.71	0.05	16.89	17.42	0.87	0.08	16.89	17.42	1.00	0.09
800	14.90	16.22	0.71	0.05	14.90	16.22	0.87	0.08	14.90	16.22	1.00	0.09

Dimensionless parameters are defined in Appendix A.

K_{lin}, dimensionless spring stiffness predicted for linear tendon properties; K_{nonlin}, dimensionless spring stiffness predicted for nonlinear tendon properties.

Appendix

Spring-mass model parameters used

The planar spring-mass model is specified by four dimensionless parameters: dimensionless spring stiffness (K), dimensionless horizontal landing velocity (U_0), dimensionless vertical landing velocity (V_0) and initial spring angle (θ_0), where $K=kl_0/M_bg$, $U_0=u_0/\sqrt{gl_0}$ (the square root of Froude number), $V_0=v_0/\sqrt{gl_0}$ and k is spring stiffness, l_0 is initial spring length, M_b is mass, g is the magnitude of the acceleration due to gravity, u_0 is horizontal landing velocity and v_0 is vertical landing velocity (McMahon and Cheng, 1990). The values of K, U_0 and V_0 that were used to simulate trotting horses of different sizes in Part 1(iv) are listed in Table A1. θ_0 was chosen so that the model bounced symmetrically, by the method described previously (Bullimore and Burn, 2006).

List of abbreviations

DDFT	deep digital flexor tendon
DF	duty factor
EMA	effective mechanical advantage
GRF	ground reaction force
MAPD	mean absolute percent deviation
M_b	body mass
RMA	reduced major axis
RPF	relative peak force
RSL	relative stride length
SDFT	superficial digital flexor tendon
SL	suspensory ligament

We thank Rachel Williams of Hartpury College, Tikki Adorian of Toyhorse International and Tracey Wilson and family for providing horses, Kelly Heath, Fiona Steel, Gina Cobb, Julie Ford and the first year Equine Science MSc students at Hartpury College (2002–2003) for technical assistance and Anne Gutmann and Kirk Holloway for helpful comments on the manuscript.

References

Alexander, R. M. and Jayes, A. S. (1983). A dynamic similarity hypothesis for the gaits of quadrupedal mammals. *J. Zool.* **201**, 135-152.

Alexander, R. M., Maloiy, G. M. O., Hunter, B., Jayes, A. S. and Nturibi, J. (1979). Mechanical stresses in fast locomotion of buffalo (*Syncerus caffer*) and elephant (*Loxodonta africana*). *J. Zool.* **189**, 135-143.

Baker, W. E., Westine, P. S. and Dodge, F. T. (1973). *Similarity Methods in Engineering Dynamics: Theory and Practice of Scale Modeling*. New Jersey: Spartan Books.

Biewener, A. A. (1989). Scaling body support in mammals: limb posture and muscle mechanics. *Science* **245**, 45-48.

Biewener, A. A. (1998). Muscle-tendon stresses and elastic energy storage during locomotion in the horse. *Comp. Biochem. Physiol.* **120B**, 73-87.

Blickhan, R. (1989). The spring-mass model for running and hopping. *J. Biomech.* **22**, 1217-1227.

Brown, N. A., Pandy, M. G., Buford, W. L., Kawcak, C. E. and McIlwraith, C. W. (2003). Moment arms about the carpal and metacarpophalangeal joints for flexor and extensor muscles in equine forelimbs. *Am. J. Vet. Res.* **64**, 351-357.

Bullimore, S. R. and Burn, J. F. (2004). Distorting limb design for dynamically similar locomotion. *Proc. R. Soc. Lond. B* **271**, 285-289.

Bullimore, S. R. and Burn, J. F. (2006). Consequences of forward translation of the point of force application for the mechanics of running. *J. Theor. Biol.* **238**, 211-219.

Donelan, J. M. and Kram, R. (2000). Exploring dynamic similarity in human running using simulated reduced gravity. *J. Exp. Biol.* **203**, 2405-2415.

Farley, C. T., Blickhan, R., Saito, J. and Taylor, C. R. (1991). Hopping frequency in humans – a test of how springs set stride frequency in bouncing gaits. *J. Appl. Physiol.* **71**, 2127-2132.

Farley, C. T., Glasheen, J. and McMahon, T. A. (1993). Running springs: speed and animal size. *J. Exp. Biol.* **185**, 71-86.

Gillis, C., Sharkey, N., Stover, S. M., Pool, R. R., Meagher, D. M. and Willits, N. (1995). Effect of maturation and aging on material and ultrasonographic properties of equine superficial digital flexor tendon. *Am. J. Vet. Res.* **56**, 1345-1350.

Griffin, T. M., Kram, R., Wickler, S. J. and Hoyt, D. F. (2004). Biomechanical and energetic determinants of the walk–trot transition in horses. *J. Exp. Biol.* **207**, 4215-4223.

Isaacson, E. and Isaacson, M. (1975). *Dimensional Methods in Engineering and Physics*. London: Edward Arnold.

Ker, R. F., Alexander, R. M. and Bennett, M. B. (1988). Why are mammalian tendons so thick? *J. Zool.* **216**, 309-324.

Koehl, M. A. R. (2004). Biomechanics of microscopic appendages: functional shifts caused by changes in speed. *J. Biomech.* **37**, 789-795.

McGuigan, M. P. and Wilson, A. M. (2003). The effect of gait and digital flexor muscle activation on limb compliance in the forelimb of the horse *Equus caballus*. *J. Exp. Biol.* **206**, 1325-1336.

McMahon, T. A. (1973). Size and shape in biology. *Science* **179**, 1201-1204.

McMahon, T. A. and Cheng, G. C. (1990). The mechanics of running: How does stiffness couple with speed? *J. Biomech.* **23**, 65-78.

Pollock, C. M. and Shadwick, R. E. (1994). Relationship between body mass and biomechanical properties of limb tendons in adult mammals. *Am. J. Physiol.* **266**, R1016-R1021.

Prothero, J. (1986). Methodological aspects of scaling in biology. *J. Theor. Biol.* **118**, 259-286.

Rayner, J. M. V. (1985). Linear relations in biomechanics: the statistics of scaling functions. *J. Zool.* **206**, 415-439.

Riemersma, D. J. and Schamhardt, H. C. (1985). In vitro mechanical properties of equine tendons in relation to cross-sectional area and collagen content. *Res. Vet. Sci.* **39**, 263-270.

Schmidt-Nielsen, K. (1984). *Scaling: Why is Animal Size so Important?* Cambridge: Cambridge University Press.

Wilson, A. M. (1991). The effect of exercise intensity on the biochemistry, morphology and mechanical properties of tendon. PhD thesis, Department of Anatomy, University of Bristol, UK.

Witte, T. H., Knill, K. and Wilson, A. M. (2004). Determination of peak vertical ground reaction force from duty factor in the horse (*Equus caballus*). *J. Exp. Biol.* **207**, 3639-3648.

Yamamoto, E., Iwanaga, W., Yamamoto, N. and Hayashi, K. (2004). Growth-related changes in the mechanical properties of collagen fascicles from rabbit patellar tendons. *Biorheology* **41**, 1-11.